Scattering of P Waves by Random Velocity Heterogeneities

AUTHOR(S):

MATSUNAMI, Koji

CITATION:

MATSUNAMI, Koji. Scattering of P Waves by Random Velocity Heterogeneities. Bulletin of the Disaster Prevention Research Institute 1981, 31(2): 59-78

ISSUE DATE:

1981-06

URL:

http://hdl.handle.net/2433/124899

Scattering of P Waves by Random Velocity Heterogeneities

By Koji MATSUNAMI

(Manuscript received March 27, 1981)

Abstract

In order to investigate the variation of spatial amplitude fluctuation with the increases of wave propagation in the medium with randomly distributed velocity heterogeneities, an ultrasonic model experiment was carried out by using perforated duralumin plate. P waves composed of several peaks and troughs was radiated from PZT compressional cylinder and was observed in the profiles transversal to the direction of wave propagation. Average amplitude level $\bar{A}$ of each phase of P wave in the profile and amplitude fluctuation δA were obtained.

From the analysis of the average amplitude level and the amplitude fluctuation, the following results were obtained: when the wavelength approachs the average size of heterogeneities, the average amplitude level attenuates remarkably with the increase of distance of wave propagation and simultaneously the amplitude fluctuation becomes intensive; variance $\sigma^2(\delta A/\bar{A})$ of fluctuation rate of amplitude, which is proportional to fluctuation rate $(\delta I/\bar{I})$ of energy flow I, increases nearly in proportion to time measured from P onset, and its growth rate per unit time depends strongly on the distance of wave propagation and the wave frequency, and from the analysis of the growth rate of variance per unit distance, these characteristics can be considered as being due to isotropic scattering; predominant length of the fluctuation, which corresponds to predominant period of oscillatory distributions of amplitudes along the profiles, is six to eight times the average size of heterogeneities, but short-period fluctuation appears in later phases.

1. Introduction.

According to the results[1] of acoustic velocity loggings carried out up to this time within the depth of about three kilometers, velocity fluctuations of seismic waves exist in the direction of depth. This suggests that heterogeneities expressed as spatial velocity fluctuations exist everywhere in the Earth's interior. According to the theory of wave scattering[2),3)], seismic wave scattering caused by the heterogeneities generates spatial fluctuations of the wave amplitude and its arrival time. Especially, when seismic waves whose wavelength are comparable to the size of heterogeneities travel long distances in the heterogeneous medium, seismic waves are strongly disturbed by the scattering effects. Therefore, the investigation of the scattering effects on seismic waves is important for accurate determination of the structure of the Earth's interior and the mechanism of earthquake source, and also gives us the clues of estimation on the fine structure of heterogeneities in the crust and upper mantle. In the case of the strong

scattering, it is very difficult to predict theoretically the variation of the spatial amplitude fluctuation with the increase of wave propagation.

Nikolayev et al. have studied the problem of seismic wave scattering by means of ultrasonic model experiments[4]. They have investigated the relation between spatial velocity fluctuation and P-wave amplitude fluctuation observed in transverse profiles, i. e. in the profiles which are transversal to the direction of wave propagation. In their experiments, duralumin plate was used as the model of the medium. In order to obtain the spatial velocity fluctuation, they have utilized the characteristic that the wave velocity in perforated duralumin plate decreases with the increase of porosity. The porosity of duralumin plate was given by small circular holes of equal diameter. The spatial fluctuation of porosity, i. e. the spatial fluctuation of velocity were made by locally varying the number of holes per each square ($2\times2cm^2$). The wave scattering in the model was generated not only by the velocity heterogeneities but also by small circular holes. Especially, in the frequency range of 180–240 KHz, the scattering effects caused by the latter can not be neglected. Therefore, in order to estimate correctly P-wave attenuation caused by the former and its amplitude fluctuation, the scattering effects caused by the latter should have been examined in detail. However, they have not been considered in their experiments.

The application of perforated duralumin plate makes it easy to obtain a heterogeneous model for experimental study on wave scattering. Therefore, a similar plate is used in our experiment to investigate the effects of strong scattering on seismic wave amplitude in accordance with Nikolayev et al's experimental procedure. According to Ivakin[5], the wave velocity in perforated plates depends on the distribution of circular holes in the plate. Further, the scattering effects caused by circular holes will be also dependent on their distribution. Therefore, in order to estimate correctly the coefficient of variation of wave velocity in the model and also to make it easy to evaluate the scattering effects by circular holes, the arrangement of circular holes within each unit of the model should be distributed uniformly in the model. In view of above, we made the model by the following method: the number of holes per each circular unit (2. 4cm in diameter) is kept constant everywhere in the model, and also the arrangement of holes within each unit is distributed uniformly everywhere in the model and the diameter of holes is varied randomly per unit.

In the experiment, P waves which are composed of several phases are observed in transverse profiles of the model. The scattering effects caused by circular holes are first examined in detail, and then P-wave amplitude fluctuation caused by the velocity heterogeneities is obtained. Mainly, the fluctuation rate of amplitude, which is the rate of amplitude fluctuation to average amplitude level along transverse profiles, is analyzed for each phase of P wave. The result shows that the variance of fluctuation rate increases nearly in proportion to time measured from the arrival of the first phase of P wave, and its growth rate per unit time within the duration of P wave depends strongly on the distance of wave propagation and the wave frequency. Further, from the analysis on the predominant length of fluctuation along transverse profile, it is shown

that the predominant length of fluctuation is much larger than the size of velocity heterogeneities, but the short-period component of fluctuation appears in the fluctuations of P-wave later phases.

2. Experimental Apparatus

The emitting and receiving apparatus are of the usual type used in model seimology. A block diagram of the apparatus is shown in **Fig. 1.** The emitter and

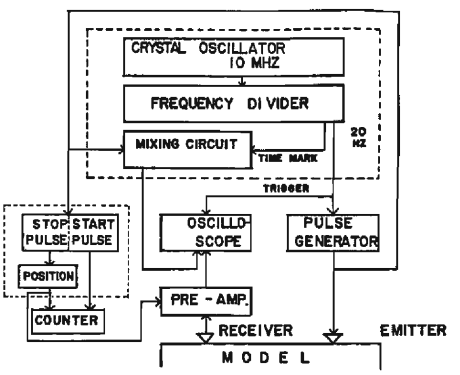

Fig. 1. Block diagram of apparatus.

receiver used in the experiment consist of a PZT compressional cylinder whose diameter is 4mm. The output pulses of the crystal oscillator with natural frequency of 10 MHz are reduced to the pulses of 1 MHz and 20 Hz by the frequency divider. The pulses of 1 MHz are used as a time mark and that of 20 Hz as a trigger pulse for the oscilloscope and the pulse generator, respectively. The counter is used for measurements of travel time. The start and stop pulses controlling the counter are made of output pulse of the pulse generator. The position of a stop pulse shaped like a spike can be controlled as we like. The stop pulse is superposed on signals in the pre-amplifier. Resolution of the counter is ± 0.1 microsecond. The pre-amplifier with imput impedance of about 2 $M\Omega$ has a gain of 40 dB within the frequency range of 6 KHz-1 MHz. The signals are observed on the oscilloscope screen and photographed by a camera. Wave velocity is determined from the travel time curves. Standard error in estimations of wave velocity is within 1%. The peak-to-peak amplitude are directly read on the scale of oscilloscope screen. Standard error in measurements of wave amplitude is within 6% when the emitter is fixed during the experiments and 9% when the emitter is reset in every measurement, respectively.

3. Characteristics of P Waves Propagating in Perforated Duralumin Plates.

When the porosity of duralumin plate is given by small circular holes with equal diameter, the wave velocity decreases with the increase of porosity[6]. We make two-

dimensional models of medium by using perforated duralumin plate. The duralumin plate used as the model is 73cm in length, 59cm in width and 0.2cm in thickness. In this section, we first obtain the relation between the wave velocity and the porosity of perforated duralumin plate made by the following method, and then examine the effects of wave scattering caused by small circular holes on P-wave amplitude. As shown in **Fig. 2**, the method of making the model is as follows: first, hexagons of 1cm in length of one side (denoted by solid and dotted ines in **Fig. 2**) are made on the surface of duralumin plate by using a net of rhombuses of 0.5cm in length of one side (solid lines), and then circular holes with equal diameter (closed circles) are made at each vertex of these hexagons and their centers by drilling. In the following, the model is called the hexagonal model for convenience. Porosity Q_c of hexagonal model is determined from the diameter of holes. **Fig. 3** shows the experimentally

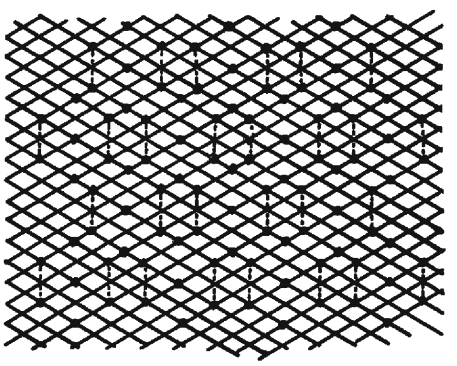

Fig. 2. Distributions of holes in perforated duralumin plates used as hexagonal models.

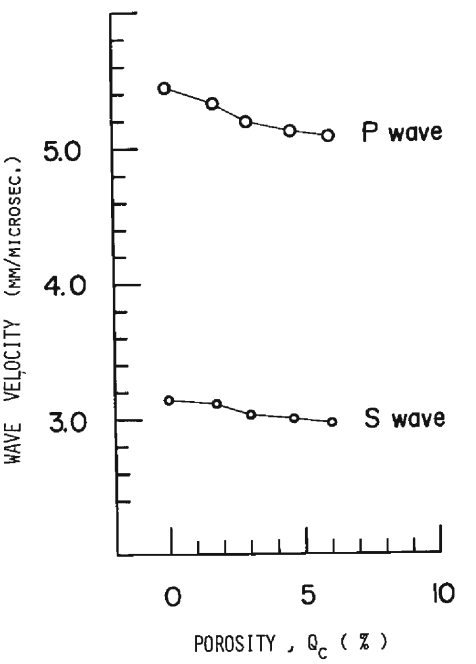

Fig. 3. Relation between the wave velocity and the porosity of hexagonal model.

Table. 1 Measured wave velocities and porosities of perforated duralumin plates used as hexagonal models.

Hexagonal Model	Porosity, Q_c in %	Diameter of Holes, D in mm.	Plate Dilatation Velocity, V_p in mm/microsec.	Shear Velocity, β in mm/microsec.
HA	0	0	5.45	3.15
HB	1.8	1.3	5.33	3.11
HC	3.0	1.7	5.21	3.03
HD	4.6	2.1	5.12	3.00
HE	6.0	2.4	5.08	2.97

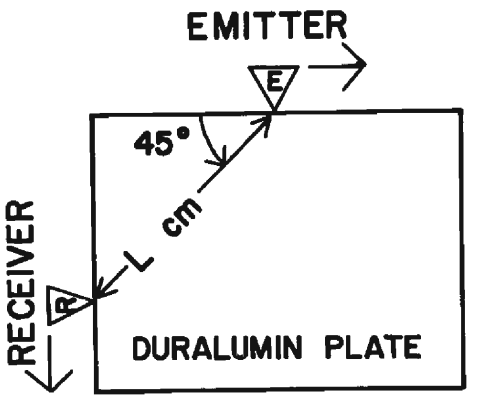

Fig. 4. Schematic diagram of the method of diagonal sounding. Emitter and receiver are simultaneously moved in the direction of arrows at the same intervel.

obtained relation between the wave velocity of the hexagonal model and its porosity. Measured wave velocities are listed in **Table 1.** When P waves travel hexagonal model, the wave amplitude should be affected by the wave scattering caused by circular holes. Therefore, we examine the scattering effects on P-wave amplitude in the following.

First, we investigate P-wave attenuation by the method of diagonal sounding[7], which is shown in **Fig. 4.** Measured amplitude is that of the first phase which is composed of the first peak and trough. It is assumed that geometrical divergence of the wave front is two-dimensional. When α denotes the attenuation coefficient of wave amplitude and L the distance of wave propagation, respectively, wave amplitude A can be written as follows: $A \propto L^{-1/2} \exp(-\alpha L)$. **Fig. 5** shows the attenuation of P-wave amplitude in model HA with no holes, hexagonal model HC with porosity of 3% and HE with porosity of 6% for various resonance frequencies f_0 of the emitter and receiver. The attenuation coefficient α_p of P-wave amplitude is determined from the inclination of the solid line denoted in the figure. **Fig. 6** shows the relation between P-wave attenuation coefficient α_p and resonance frequency f_0. As can be seen in **Fig. 6,** attenuation characteristics of P waves are as follows: in the case of resonance frequency which is higher than 200 KHz, the difference between the attenuation coefficient of model HA with no holes and those of hexagonal models becomes significant, but within the resonance frequency range of 86-150 KHz, the attenuation coefficients are almost the same for all models. Accordingly, P-wave attenuation which is due to the wave scattering caused by circular holes can be neglected within the resonance frequency range of 86-150 KHz for hexagonal models with porosity which is less than 6%.

Secondly, we examine the spatial stability of P-wave form observed in transvease profiles, i. e. in the profiles which are transversal to the direction of wave propagation. **Fig. 7** shows a schematic diagram based on observation of P waves in transverse profiles of the model. Measurements in profile II are carried out in the following

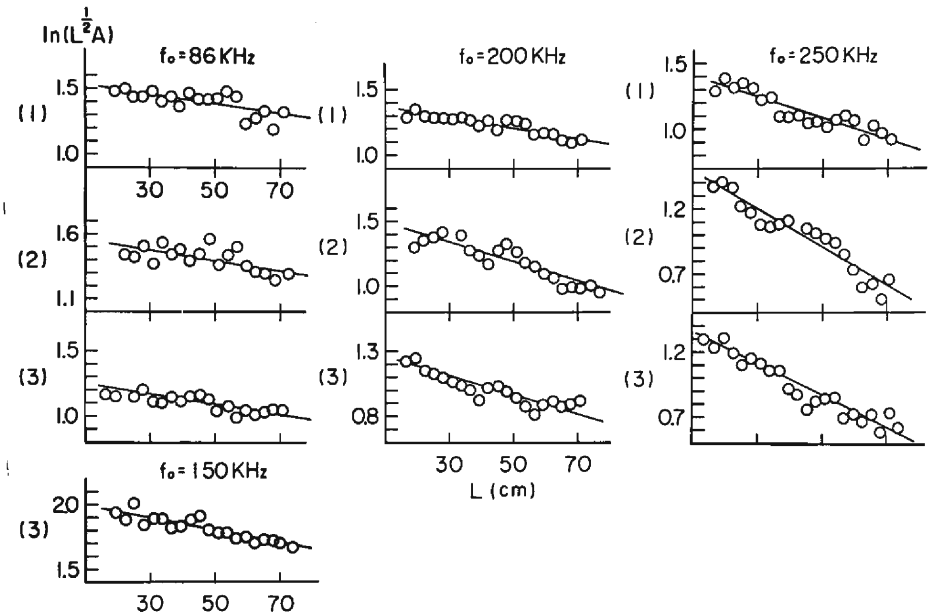

Fig. 5. Attenuation of the natural logarithms of P-wave amplitude with distance L. Values of amplitudes are corrected for geometrical divergence of wave front. Solid lines are obtained by the least square method. (1) : model HA with no holes, (2) : hexagonal model HC with Q_c of 3%, (3) : hexagonal model HE with Q_c of 6%.

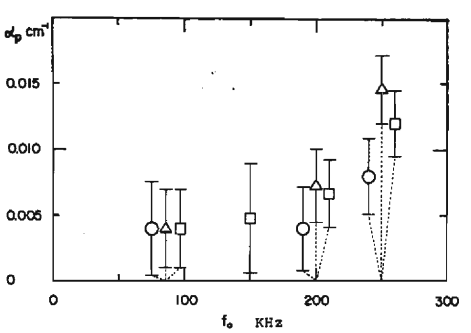

Fig. 6. Relation between attenuation coefficient α_f and resonance frequency f_0. Each symbol denotes the following cases : (○)-model HA with no holes, (△)-hexagonal model HC with Q_c of 3%, (□)-hexagonal model HE with Q_c of 6%. Error bars denote the 95% confidence limits.

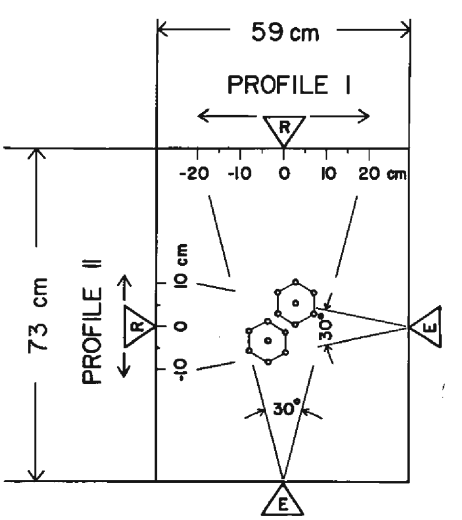

Fig. 7. Schematic diagram of observations.

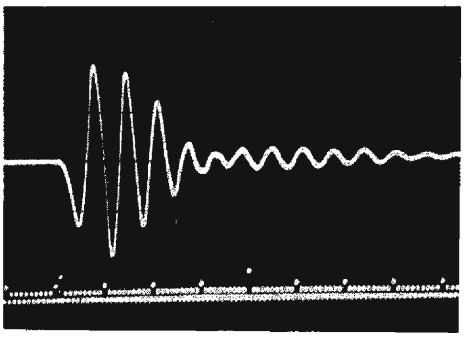

Photo. 1. Original waveform in the case of $f_0=150$ KHz.

way; the emitter is fixed in the middle of one of the long edges of the model; the receiver is moved at intervals of 1cm along the other long edges in which the angle of incidence is within the range of 0-15°. Measurements in profile I are also carried out along short edges of the model by the same method as in profile II. Average distance L of wave propagation is 60 cm and 74 cm, in the case of profile II and profile I, respectively. Accordingly, it can be considered that both profiles run parallel to the wave front. **Photo.1** shows original waveform obtained by directly contacting the receiver with the emitter of $f_0=150$ KHz. The original waveform is composed of three main phases. **Photo.2** shows the examples of records observed in profile of hexagonal model HC for $f_0=150$ KHz where P-wave attenuation by the wave scattering caused by circular holes is negligible. **Fig. 8** shows amplitude distributions along the profile for each phase of P waves which are shown in **Photo. 2**. It is clear from this figure that the amplitude distribution along the profile is almost flat for all phases. Accordingly, it can be considered that the amplitude distribution along transverse

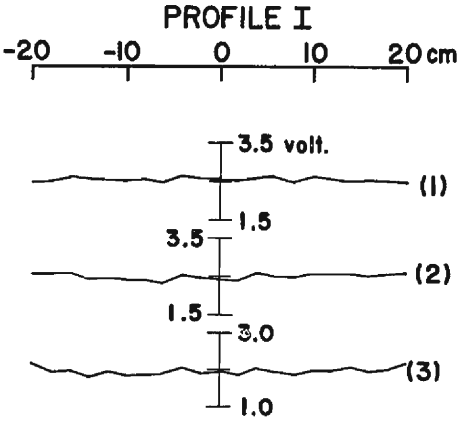

Fig. 8. Amplitude distribution along profile I for each phase of P wave. Measured amplitude is from peak-to-peak. (1) : the 1st phase composed of the 1st peak and trough of a P wave, (2) : the 2nd one, (3) : the 3rd one.

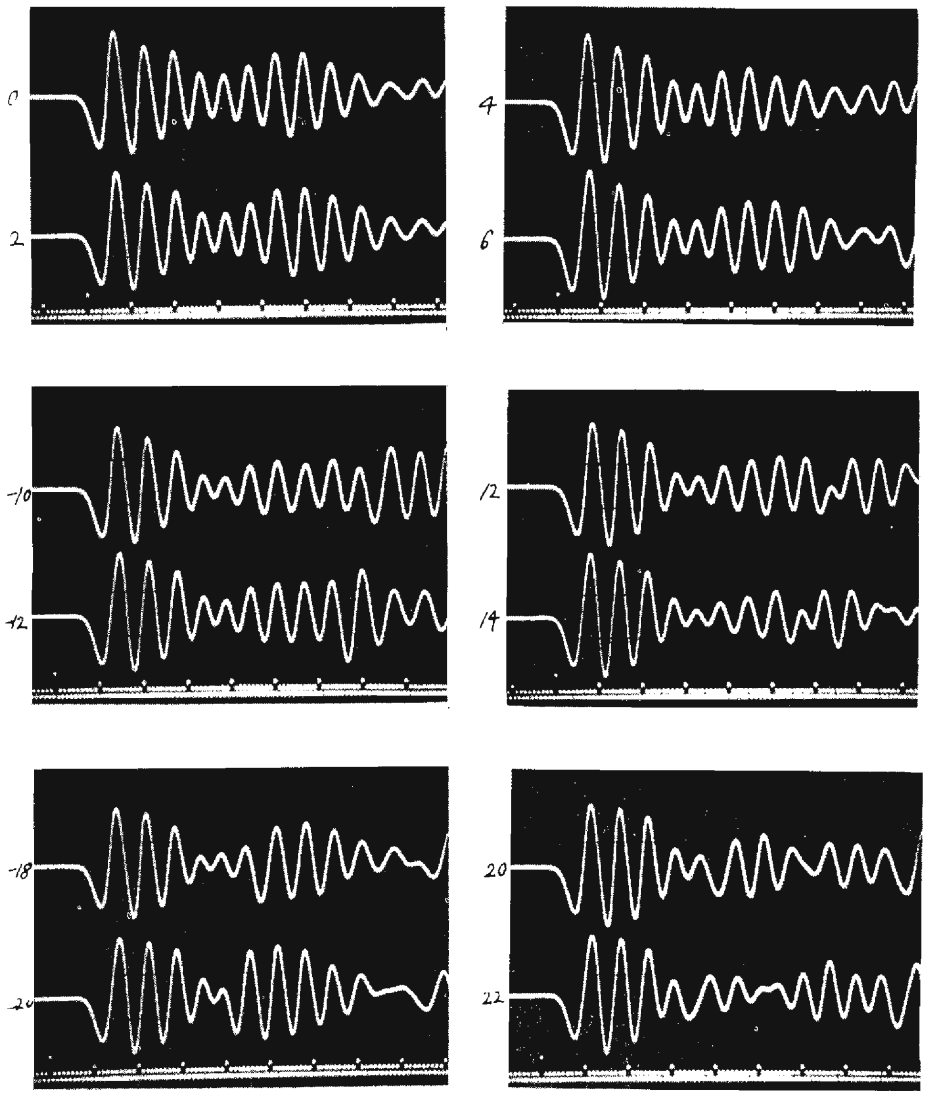

Photo. 2. Examples of records observed in profile I of hexagonal model HC in the case of $f_0=150$ KHz.

profile is almost flat when P waves are not affected by wave scattering. In the following, we regard the average value of amplitude over the profile as an average amplitude level $\bar{A}$. On the assumption that amplitude $A(x)$ observed at arbitrary point x in the profile is composed of determined component expressed by average level $\bar{A}$ and random one expressed by fluctuation $\delta A(x)$, we can write $A(x)$ as follows: $A(x)=\bar{A}+\delta A(x)$. It is reasonable to examine the fluctuation rate $(\delta A/\bar{A})$ of amplitude along the profile in order to compare the degree of spatial variation of amplitude among different phases or different waves. **Fig. 9** shows the fluctuation rate

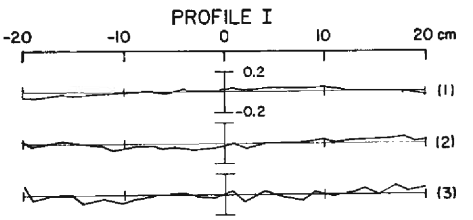

Fig. 9. Distribution of fluctuation rate $(\delta A/\bar{A})$ along profile I for each phase of a P wave. (1) : the lst phase, (2) : the 2nd one, (3) : the 3rd one.

along the profile for each phase of P waves which are shown in **Photo. 2.** The coefficient of variation of amplitude, i. e. $\sigma(\delta A/\bar{A})$ is estimated to be less than 6% for all phases of P waves which are shown in **Fig. 9.**

From the above examinations, we can conclude that P-wave amplitude attenuation by the wave scattering caused by circular holes is negligible within the resonance frequency range of 86-150 KHz for a hexagonal model whose porosity is less than 6%, and as a result, the amplitude fluctuation along transverse profile is also negligible

4. Characteristics of P Waves Propagating in a Model of Medium with Randomly Distributed Velocity Heterogeneities.

In the previous section, we obtained the relation between the wave velocity and the porosity of the hexagonal model, and confirmed that the effects of wave scattering caused by circular holes in the hexagonal model on P-wave amplitude were negligible within the resonance frequency range of 86-150 KHz for a hexagonal model whose porosity is less than 6%. In this section, we first made a model of a medium with randomly distributed velocity heterogeneities on the basis of the results of the previous section, and then investigated the characteristics of P waves propagating in the heterogeneous model.

4-1. A Model of a Medium with Randomly Distributed Velocity Heterogeneities.

We made the model of a medium with randomly distributed velocity heterogeneities in the following way: as shown in **Fig. 10**, when the diameters of holes of hexagonal model are randomly varied from one hexagon to another, the porosity of the unit surrounded by a circle of about 2. 4cm in diameter varies also randomly from one unit to another, and therefore the wave velocity varies also randomly. The range of randomly distributed porosities is 0-6% and the median is 3%. P-wave velocities of the unit with some porosities are determined from the relation shown in **Fig. 3** and those are listed in **Table 2.** Diameter 2. 4cm of the unit can be considered as the average size of velocity heterogeneities. In the following, we call the model random model RA. As listed in **Table 2**, average value $\bar{V}_p$ of P-wave velocity in random

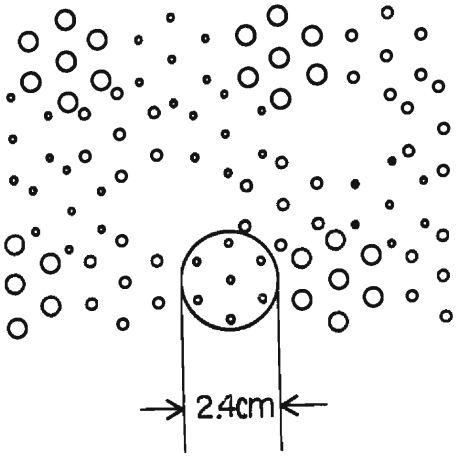

Fig. 10. Distribution of holes in random model RA.

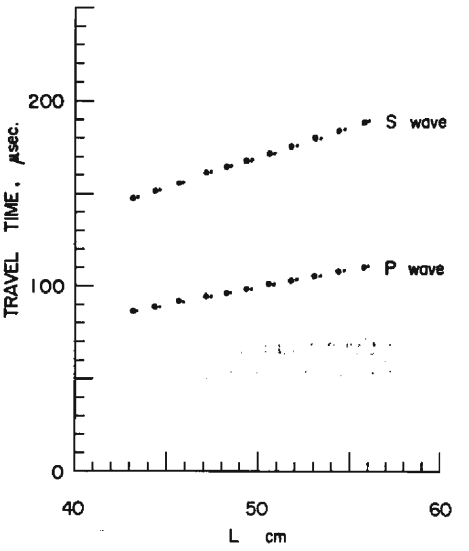

Fig. 11. Travel time curves of P and S waves observed in random model RA (●) and hexagonal model HC (•).

Table 2. List of the units distributed in random model RA.

Q_c (%)	D (mm)	V_p (mm/microsec.)	Number of Units, N
0	0	5.45	63
1.0	1.0	5.39	82
1.3	1.1	5.36	84
1.8	1.3	5.33	87
2.3	1.5	5.28	85
3.0	1.7	5.21	82
3.4	1.8	5.18	85
4.2	2.0	5.14	84
4.6	2.1	5.12	73
5.5	2.3	5.09	85
6.0	2.4	5.08	70
3.0 (Average)	1.7 (Average)	5.21 (Average)	880 (ΣN)

model RA is 5.21 mm/microsecond and the coefficient of its variation, i. e. $\sigma(\delta V_p/\bar{V}_p)$ is 2.4%.

Fig. 11 shows the travel time curves for P and S waves observed in random model RA and hexagonal model HC whose porosity is equal to that of random model RA. It is clear from this figure that the wave velocities of both models are almost the same. This indicates that the wave velocity in a perforated duralumin plate is well controlled by the porosity given by small circular holes.

4-2. P-Wave Scattering in Random Model RA.

In random model RA, the velocity heterogeneities caused by the unit of 2.4cm in diameter are randomly distributed. When P wave travels the model, it should be scattered by the heterogeneities. In order to confirm the generation of the wave scattering caused by the velocity heterogeneities, we examine the average level of P-wave amplitude and its fluctuation observed in transverse profiles of random model RA for the resonance frequency range of 86-150 KHz. As shown previously, the scattering effects caused by circular holes can be neglected in this frequency range. The procedure of measurements in random model RA is just the same as in hexagonal models and also its schematic diagram is shown in **Fig.7**. **Photo.3** shows the examples of P-wave forms observed in profile I of random model RA for $f_0=150$ KHz. The waveforms are unstable when compared with those observed in hexagonal model HC,

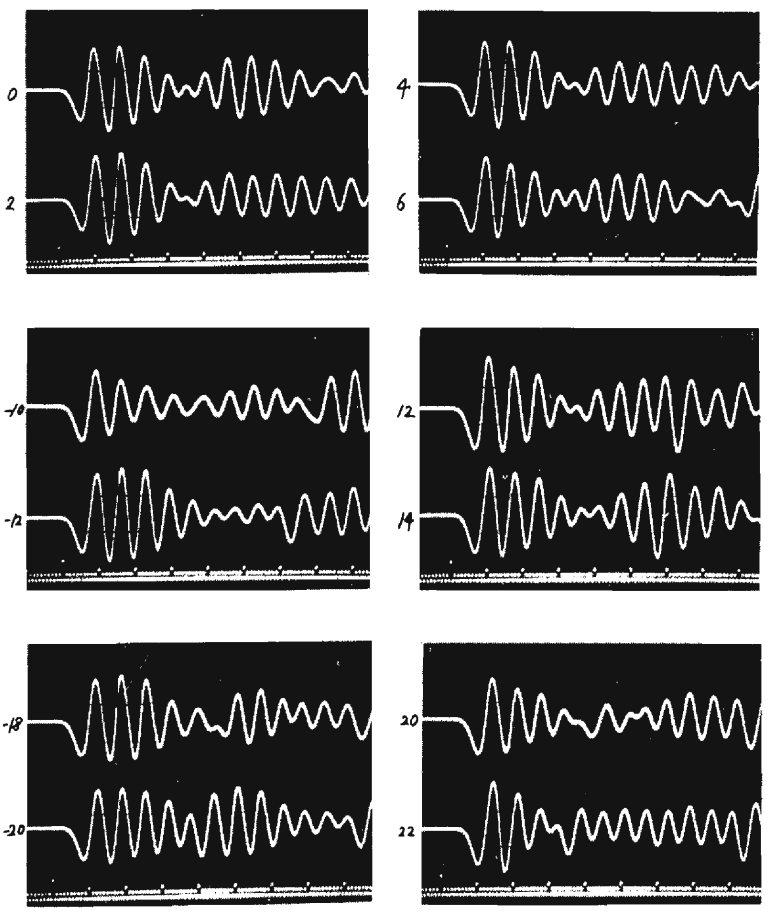

Photo. 3. Examples of records observed in profile I of random model RA in the case of $f_0=150$ KHz.

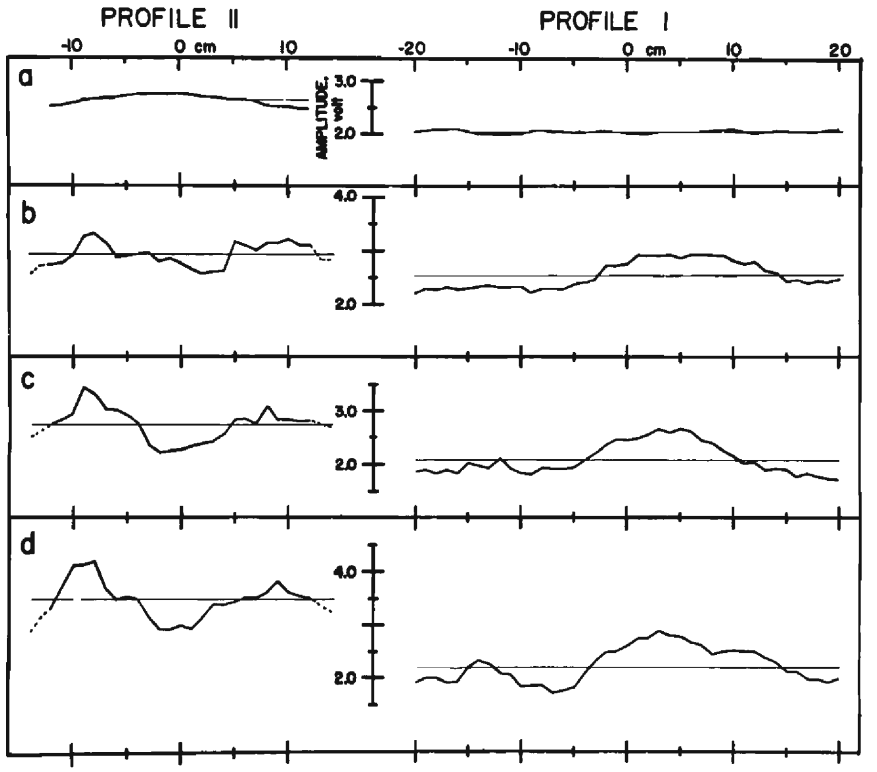

Fig. 12. Amplitude distribution of the first phase of P wave along profile II and I in the following cases: (a)-hexagonal model HC with Q_c of 3% for f_0=150 KHz, (b), (c) and (d)-random model RA for f_0=86 KHz, 110 KHz and 150 KHz, respectively. Note that the attenuation of average level $\bar{A}$ in case (d) is very large compared with that in case (a).

and the instability becomes larger in later phases of P wave. **Fig. 12** shows the amplitude distributions of the first phases of P waves along profile II and I for f_0= 86 KHz, 110 KHz and 150 KHz. In this figure, average level $\bar{A}$ is denoted by flat lines. The average distance L of wave propagation is 60 cm and 74 cm, in the case of profile II and I, respectively. As may be seen from this figure, the main characteristics of the average level and the fluctuation are as follows: the average level attenuates remarkably for higher resonance frequency with the change of profile from II to I; the degree of fluctuation becomes larger for higher resonance frequency in both profiles but almost does not vary for all frequencies with the change of profile from II to I; the shape of fluctuation is similar for all resonance frequencies in the same profile; the predominant length of fluctuation is about 13-18cm in both profiles. From among the above characteristics, we especially investigate the attenuation of average level and the root mean square (rms) of fluctuation, i. e. $\sigma(\delta A)$ with the change of profile from II to I, i. e. with the increase of distance of wave propagation, and later

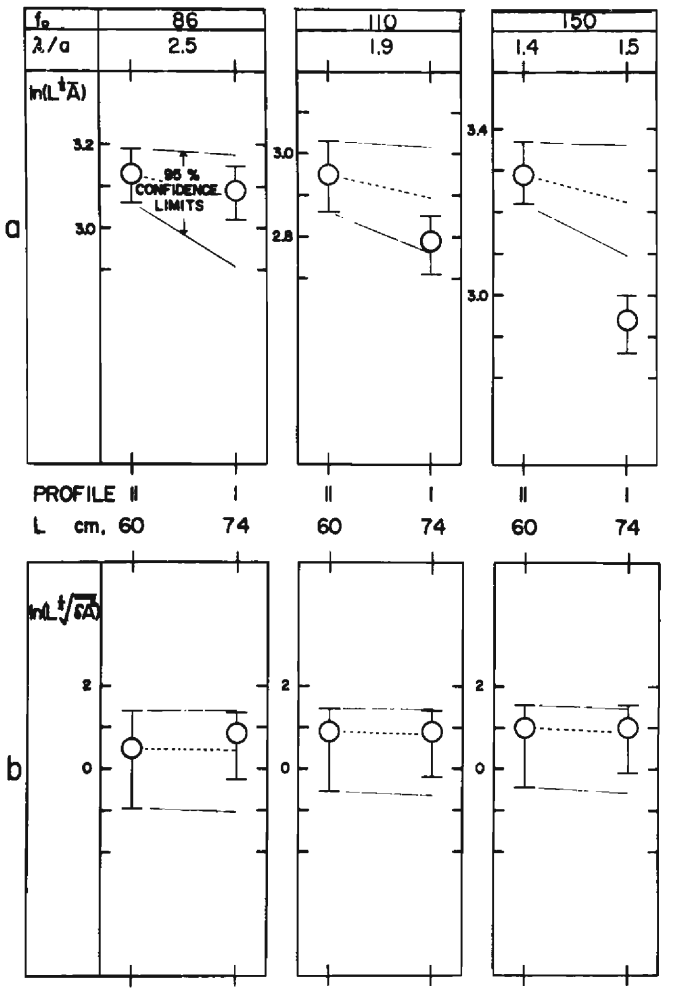

Fig. 13. Attenuation of the natural logarithms of average level $\bar{A}$ (a) and rms fluctuation $\sigma(\delta A)$ (b) with distance L. Values of amplitudes are corrected for geometrical divergence of wave front.

investigate the rest of the above. **Fig. 13** shows the attenuation for each resonance frequency. When it is assumed that the attenuation coefficient of P-wave amplitude in random model RA is the same as in hexagonal model HC whose porosity is equal to that of random RA, the expected 95% confidence limits of attenuation are the lines denoted by arrows in this figure and the mean values by dotted lines, respectively. As can be seen in this figure, when the ratio (λ/a) of predominant wavelength to average size of heterogeneities is 2. 5, the average level is within the confidence interval but it entirely goes out when the ratio becomes 1. 4 to 1. 5. Rms $\sigma(\delta A)$ of fluctuation does not significantly attenuate. From the attenuation of average level with

the approach of ratio (λ/a) to unity and the simultaneous increase of fluctuation, it is considered that P-wave scattering caused by the velocity heterogeneities is generated in random model RA. The small attenuation of rms $\sigma(\delta A)$ is reasonable, because a random component is newly generated by the scattering of the determined one and also remains the same even if it were scattered.

5. Fluctuation Characteristics of P-Wave Amplitude.

Generally, the wave is scattered equally in all directions when the ratio (λ/a) of predominant wavelength to average size of heterogeneities is much larger, and is sharply scattered in the direction of propagation of the incident wave when the ratio is much smaller. When incident P wave is composed of several peaks and troughs, the amplitude fluctuation becomes larger in later phases for the case of the former and is the same in all phases for the case of the latter, respectively. In such a range of ratio (λ/a) from 1. 4 to 2. 5, as in our experiment, the directivity of scattering can not

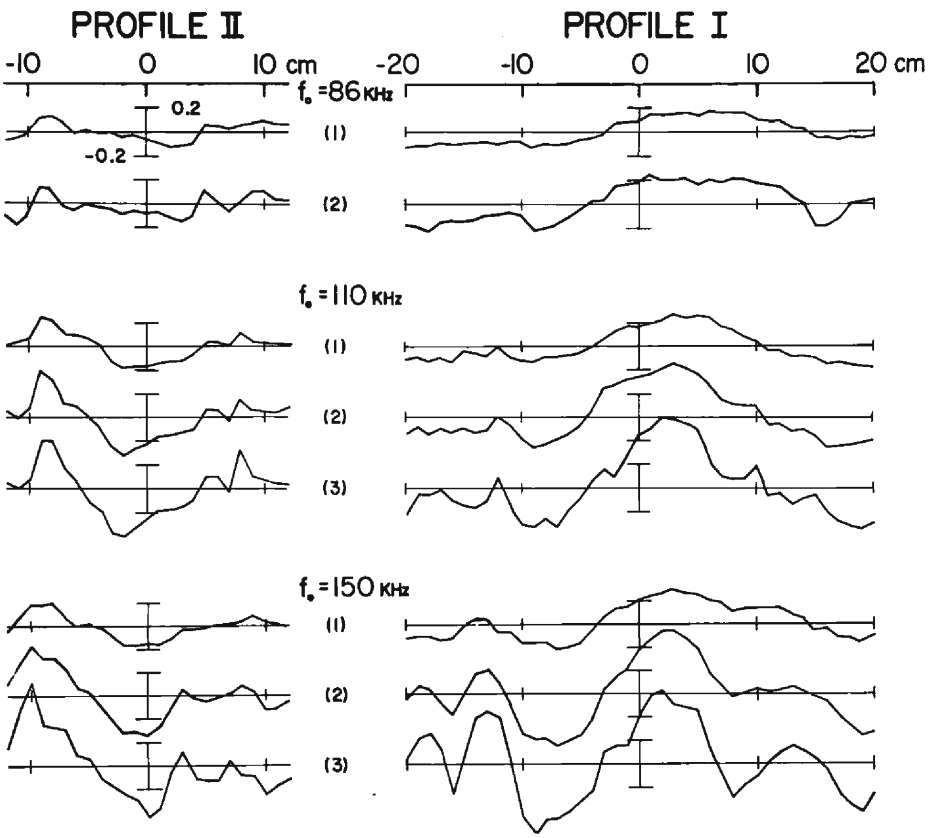

Fig. 14. Distribution of fluctuation rate $(\delta A/\bar{A})$ along profile II and I. (1) : the lst phase, (2) : the 2nd one, (3) : the 3rd one.

be predicted theoretically. Accordingly, we equally investigate the amplitude fluctuation of each phase of P wave. We measure the peak-to-peak amplitude of each phase of a P wave, and calculate fluctuation rate $(\delta A/\bar{A})$ along the profile for each phase of P wave. **Fig. 14** shows the fluctuation rate along profile II and I for each resonance frequency. As is clear from this figure, the main characteristics of the fluctuation are as follows: (1) the shape of fluctuation along the profile is almost the same for all phases in all cases of resonance frequency but the shape in profile II differs from that in profile I; (2) the fluctuation rate becomes larger in later phases; (3) the predominant length of fluctuation is much larger than the average size of velocity heterogeneities, but the short-period component of fluctuation appears in later phases, and this characteristic becomes especially remarkable for $f_0 = 150$ KHz. Characteristic (1) has also been reported by Nikolayev et al.[4], therefore, we especially investigate characteristic (2) and (3) in the following.

5-1. Intensity of Fluctuation Rate $(\delta A/\bar{A})$.

The increase of fluctuation rate $(\delta A/\bar{A})$ in later phases produces the following result: fluctuation rate $(\delta I/\bar{I})$ of energy flow I increases with time within the duration of P wave. In order to make this characteristic clear, we examine the relation between variance $\sigma^2(\delta A/\bar{A})$ and time τ measured from P onset as shown in **Fig. 15.** In this figure, variance $\sigma^2(\delta A/\bar{A})$ for each phase is respectively plotted at the point

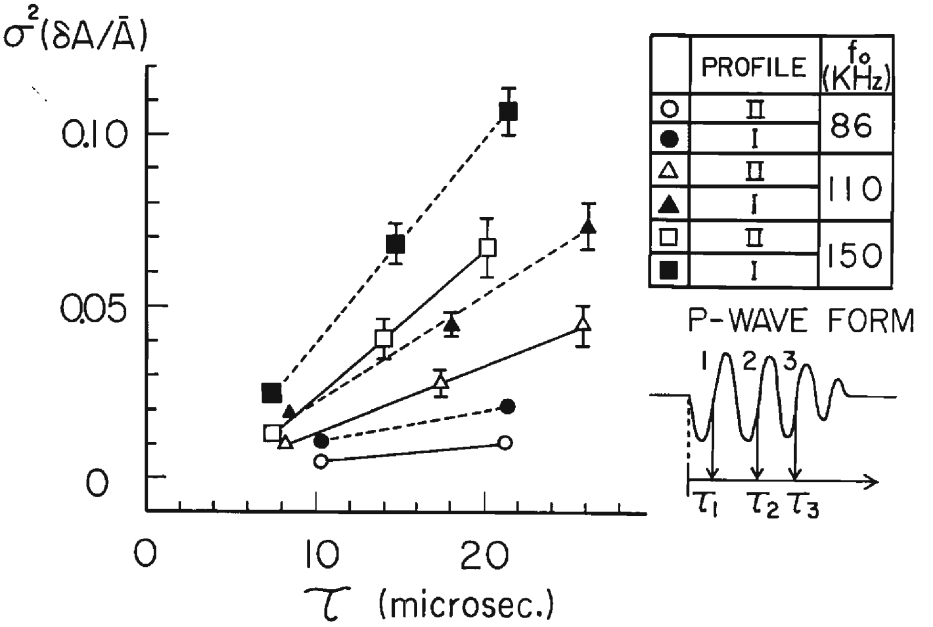

Fig. 15. Relation between variance $\sigma^2(\delta A/\bar{A})$ and time τ. Solid lines denote cases of profiel II and dotted lines cases of profile I, respectively. Error bars denote the standard deviations.

when each phase crosses zero level. As may be seen from this figure, when τ is larger than τ_1, the variance seems to increase in proportion to τ in both profiles. When we roughly estimate the growth rate of variance per unit time from the inclination of the line measured by eye in this figure, it is larger for higher resonance frequency in both profiles, and also larger in profile I than in profile II for the same resonance frequency. It is considered that the difference between the growth rate in profile II and that in the profile I for the same resonance frequency is due to the difference of distance L of wave propagation. Thus, the growth rate strongly depends on the wave frequency and the distance of wave propagation, therefore, when P wave composed of several phases travels through the medium with randomly distributed velocity heterogeneities, the distortion of waveform by wave scattering is larger in later phases of P wave, and the growth rate of distortion with the increase of distance of wave propagation is also larger. Furthermore, these characteristics become more remarkable as ratio (λ/a) approachs unity.

In order to investigate the cause of the dependency of the growth rate per unit time on distance L, we examine the relation between variance $\sigma^2(\delta A/\bar{A})$ and distance L. **Fig. 16** shows the relation for each phase. In this figure, the variance of each phase in profile II and I are connected by a dotted line in order to compare the degree of the increase of variance among different phases of a P wave. As can be seen clearly in the figure, the inclination of the line becomes larger for later phases in all cases of resonance frequency, and it is especially notable that all lines cross the axis of abscissa at the point $L\cong$40cm. This latter characteristic indicates that the variance of any phase depends on distance L in the same manner, and suggests that the wave can be considered as being a plane wave in the case of $L>$40cm. Accordingly, on the assumption that variance $\sigma^2(\delta A/\bar{A})$ of any phase increases in proportion to distance L, the growth rate of variance per unit distance is estimated

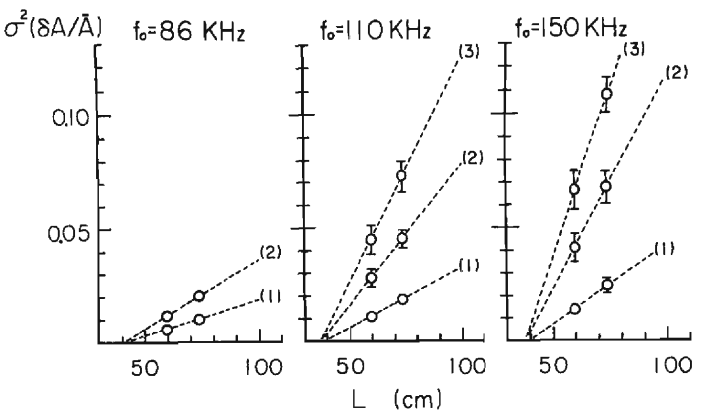

Fig. 16. Relation between variance $\sigma^2(\delta A/\bar{A})$ and distance L. (1) : the lst phase, (2) : the 2nd one, (3) : the 3rd one. Note that all dotted lines cross the axis of abscissa at the polnt of about 40cm.

Table 3. Growth rate of variance $\sigma^2(\delta A/\bar{A})$ per unit distance.

$g_i(\mathrm{cm}^{-1})$	Resonance Frequency, f_0		
	86 KHz	110 KHz	150 KHz
g_1	0.00043 ± 0.00003	0.00071 ± 0.00005	0.00085 ± 0.00006
g_2	0.00071 ± 0.00006	0.00121 ± 0.00009	0.00193 ± 0.00009
g_3		0.00200 ± 0.00017	0.00286 ± 0.00022

from the inclination of the dotted line. The obtained growth rates are listed in **Table 3.** In this table, g_i denotes the growth rate of the ith phase of P wave, and upper and lower values are within 90% confidence limits. From this table, the following equation may exist for any resonance frequency: $g_1 \simeq g_2/2 \simeq g_3/3$. This relation can be explained by the following process of wave scattering. When the average amplitude level of each phase is not so different and the scattering is also isotropic, the amplitude fluctuation of the first phase is generated by its own phase scattered forward, and those of the second and third phases are generated by their own phases scattered forward and by the preceding phases scattered backward. In these processes, it is predicted that there is the equation of $g_1 \simeq g_2/2 \simeq g_3/3$ among the growth rates of different phases. Accordingly, it is considered that isotropic scattering is generated in our experiment. As a result, the growth rate of variance per unit time depends on distance L. Further, it is clear from **Table 3** that the growth rate is larger for higher resonance frequency. This reflects the dependency of scattering coefficient on wave frequency.

According to Nikolayev[3], growth rate g_1 of the first phase is equivalent to turbidity coefficient g, i. e. the rate of forward scattered energy to total scattered energy per unit distance of wave propagation. In our experiment, we measured P-wave amplitude in the direction of wave propagation, therefore, it is considered that forward scattered P waves mainly contribute to the observed fluctuation of P-wave amplitude. If we can obtain the scattering coefficient of a P wave, we can roughly estimate the rate of forward scattered P-wave energy to total scattered energy from the ratio (g/α_p) of turbidity coefficient g to scattering coefficient α_p. The scattering coefficient can be roughly estimated from the attenuation of average amplitude level, which is shown in **Fig. 13.** The obtained ratio (g/α_p) is about 0.06 for $f_0=110$ KHz and about 0.04 for $f_0=150$ KHz, respectively. This indicates that only a very fractional part of the scattered energy contributes to the fluctuation of P-wave amplitude, and also suggests that it is necessary to consider the scattering process with conversion of wave type in order to explain the energy loss by wave scattering[8]. Further, the obtained ratio (g/α_p) decreases with resonance frequency. This tendency is in contradiction to theoretical prediction, therefore, it is necessary to examine in detail by using various models in wide range of resonance frequency.

5-2. Predominant Length of Fluctuation.

According to the theory of wave scattering[2], the average size of randomly distributed heterogeneities is roughly estimated from predominant length of transverse amplitude fluctuation. As shown in **Fig. 12**, the predominant length obtained in the experiment is about 13 to 18cm for the first phase in both prosiles, and it is six to eight times the size of heterogeneities. As can be seen in **Fig. 14**, the shorter-period fluctuation, when compared with that of the first phase, appears in later phases. The obtained predominant length of amplitude fluctuation is very great when compared with the size of heterogeneities, but it becomes shorter in later phases. A characteristic similar to the latter has been also reported by Strizhkov[9], who has experimentally investigated amplitude characteristics of P waves propagating in the model of a medium with randomly distributed cracks.

The obtained characteristics can not be predicted from the theory of wave scattering. But it is necessary to examine further these characteristics by using various models with different degrees of heterogeneity, because the above results were obtained from an experiment in which only one random model was used.

6. Conclusion.

We experimentally investigated the amplitude characteristics of P wave which travels through the model of a medium with randomly distributed velocity heterogeneities whose size are comparable to the wavelength. Though the experimental procedure is almost in accordance with Nikolayev et al's one[4], our experiment differs from theirs in the following point: first, we examined the effects of wave scattering caused by circular holes on P-wave amplitude, and then carried out the experiment on the wave scattering caused by the velocity heterogeneities in the frequency range where the scattering effects by circular holes are negligible. As a result, we could draw conclusions on the pure effects of the wave scattering caused by the velocity heterogeneities on P-wave amplitude. The main experimental results are as follows.

(1) When ratio (λ/a) of wavelength to the average size of velocity heterogeneities approachs unity, average level of amplitude attenuates remarkably with increase of wave propagation and also its fluctuation becomes intensive. These are the scattering effects caused by the velocity heterogeneities.

(2) Variance $\sigma^2(\delta A/\bar{A})$, which is proportional to fluctuation rate $(\delta I/\bar{I})$ of energy flow I, increases nearly in proportion to time within the duration of a P wave, and the growth rate per unit time depends strongly on the distance of wave propagation and the wave frequency. From the analysis of the growth rate of variance per unit distance of wave propagation, these characteristics can be considered as being due to isotropic scattering. From the ratio (g/α_p) of turbidity coefficient to scattering coefficient, the rate of energy contributing to amplitude fluctuation to total scattered

energy is estimated to be the order of 10^{-2}. This indicates that it is necessary to consider the scattering process with conversion of wave type, i. e. P-S scattering, in order to explain the energy loss by P-wave scattering.

(3) The predominant length of the amplitude fluctuation along transverse profile is six to eight times the average size of velocity heterogeneities, but short-period fluctuation appears remarkably in later phases.

The coefficient of variation of P-wave velocity in the model used is 2.4%, and it also exists in real medium according to the results of acoustic velocity loggings. Result (1) indicates the following matter: when short-period seismic waves whose wavelength are comparable to the size of heterogeneities travel through the medium with local velocity heterogeneities, the wave amplitude attenuates very remarkably with the increase of distance of wave propagation by the wave scattering caused by the heterogeneities, and simultaneously the amplitude fluctuation is generated strongly. Result (2) suggests that the distortions of P-wave form with the increasing distance of its path are found first at its latest phase and shift to earlier phase of the P wave and finally the entire form is destroyed. Further, it is suggested from result (1) and (2) that main process of wave scattering is isotropic scattering with conversion of wave type when ratio (λ/a) approachs unity. Result (3), which shows some differences from theoretical predictions, must be examined further by using different models.

P-wave isotropic scattering with conversion of wave type is to be examined by using different models in a next paper, and also the relation between amplitude fluctuation and the average size of heterogeneities, the effects of scattered waves on P coda and S-wave scattering caused by velocity heterogeneities are to be studied in future.

Acknowledgement

The author wishes to express his sincere thanks to Prof. Soji Yoshikawa of Kyoto University for his encouragement, and also to Mr. Junpei Akamatsu for his very valuable discussions in carrying out this work. The author is indebted to Messrs. Masao Nishi and Toshio Kobayashi for their helpful assistance with experiments and to Miss Kazue Segawa for her help.

References

1) Епинатъева, А. М.: Скоростъ Распространения Сейсмических Волн в Кристалических и Метаморфических Породах, Изв. АН СССР. физика Земли, № 2, 1975.
2) Chernov, L. A.: Wave Propagation in a Random Medium, McGraw-Hill, New York, 1960.
3) Николаев, А. В.: Сейсмика Неоднородных и Мутных Сред, Наука, М., 1972.
4) Николаев, А. В. и А. Г. Аверъянов : Исследование Амплитуд Продолъных Волн в Плоской Модели Среды со Случайными Флуктуациями Скорости, Изв. АН СССР. Физика Земли, № 5, 1973.
5) Ivakin, B. N.: Methods for Controlling the Density and Elasticity of a Medium During the

Two-Dimensional Modeling of Seismic Waves, Izv., Geophys. Ser., 1960, pp. 761-771.
6) Ivakin, B. N. and YU. V. Vasil'ev: The Wave Properties of Perforated Plates for Seismic Modeling, Izv., Geophys. Ser., 1963, pp. 248-260.
7) Коган, С. Я.: Сейсмическая Энергия и Методы ее Определения, Наука, М., 1975.
8) Knopoff, L. and J. A. Hudson: Scattering of Elastic Waves by Small Inhomogeneities, J. Acoust. Soc. Amer., Vol. 36, No. 2, 1964.
9) Стрижков, С. А.: Моделъные Исследования Волнового Поля в Случайно Трещиноватой Среде, Изв. АН СССР. физика Земли, № 6, 1979.